# Reaction mechanism of acetylene hydrochlorination on defective carbon supported ruthenium catalysts by DFT calculations and experimental approaches

Xiaolong Wang,[a] Dong Fan,[b] Guojun Lan,[a] Zaizhe Cheng, [a] Xiucheng Sun, [a] Yiyang Qiu,[a] Wenfeng Han,[a] Haodong Tang,[a] Huazhang Liu,[a] Yihan Zhu,[a] Xiaojun Hu,[*,b] and Ying Li[*,a]

[a] Institute of Industrial Catalysis, Zhejiang University of Technology, Hangzhou ChaoWang Road 18, 310032, PR China
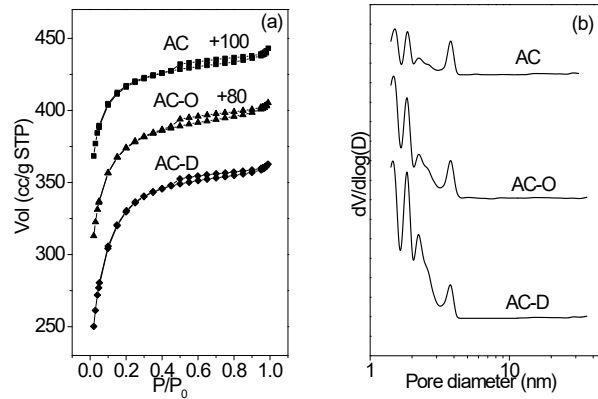
[b] College of Materials Science and Engineering, Zhejiang University of Technology, Hangzhou ChaoWang Road 18, 310032, PR China
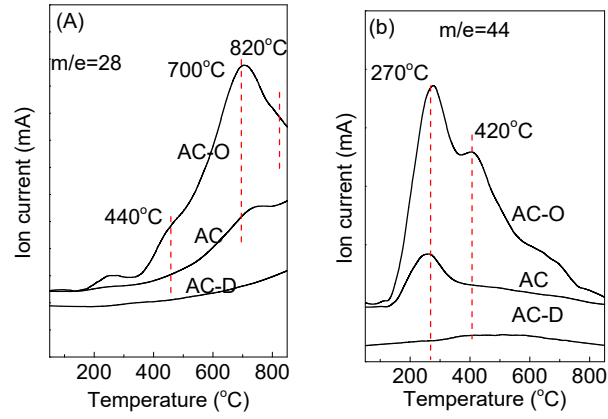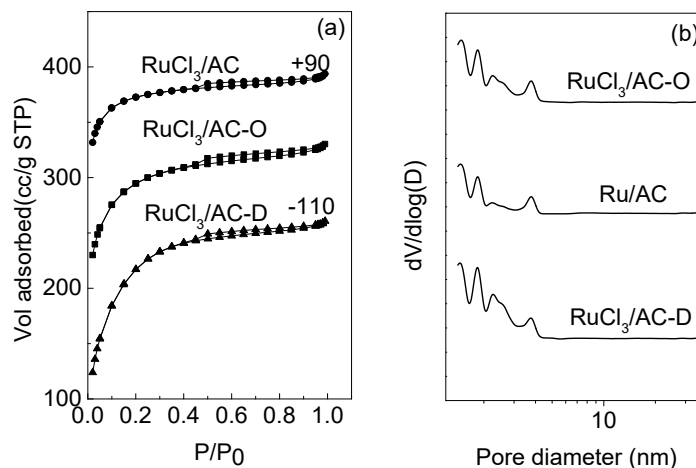
Figure S1 Argon temperature programmed desorption profile of AC, AC-O, and AC-D (a) CO_2 evolution ion and (b) CO evolution.
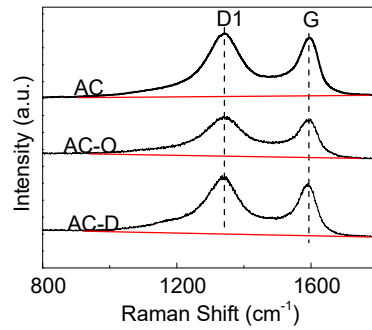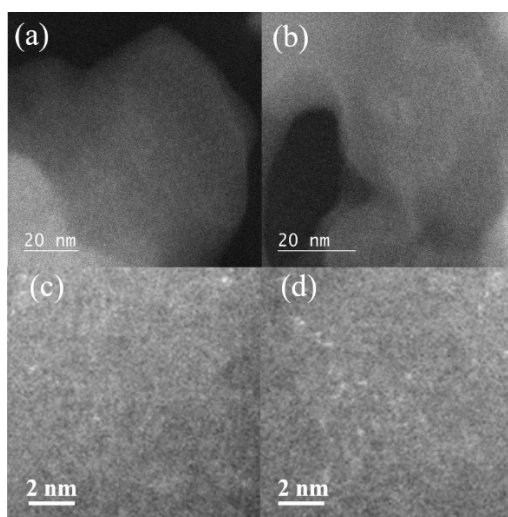

**Figure S2.** Raman spectra of AC, AC-O and AC-D

Figure S3. (a) Nitrogen adsorption-desorption isotherms and (b) pore size distributions for AC, AC-O, and AC-D.
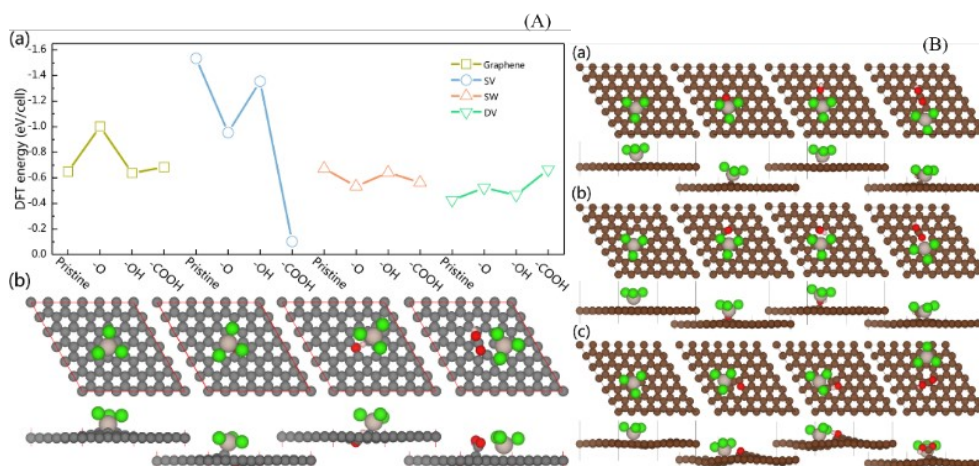
Figure S4. (a) Nitrogen adsorption-desorption isotherms and (b) pore size distributions for ruthenium catalysts.


Figure S5. HAADF-STEM images of RuCl$_3$/AC and RuCl$_3$/AC-O at low magnifications (a), (b) and high magnifications (c), (d), respectively.
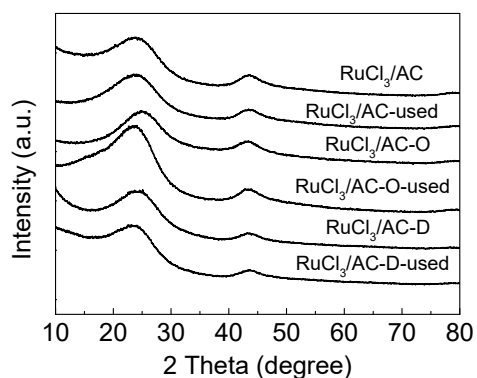

Figure S6. X-ray powder diffraction (XRD) of fresh and used RuCl$_3$/AC, RuCl$_3$/A-O and RuCl$_3$/AC-D

Figure S7. (A) Calculated adsorption energy for different defective structures (with different functional groups): pristine graphene, single vacancy (SV), double vacancy (DV), and Stone–Wales (SW) vacancy structures for (a) and the crystal structures of single vacancy (SV). The modification of different functional groups is also considered, from left to right: pristine, modified with -O, -OH, and -COOH groups, respectively for (b). (B) Relaxed geometries for different $RuCl_3$ adsorbed systems. Top view (upper) and side (lower) view of the $RuCl_3$ adsorbed (a) pristine graphene, (b) DV, and (c) SW structures. The modification of different functional groups is also considered, from left to right: pristine, modified with -O, -OH, and -COOH groups, respectively.
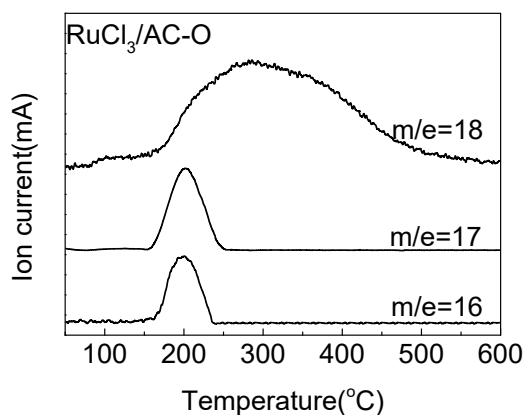
Figure S8. Ammonia temperature programmed desorption (NH_3-TPD) profiles of $RuCl_3$/AC-O
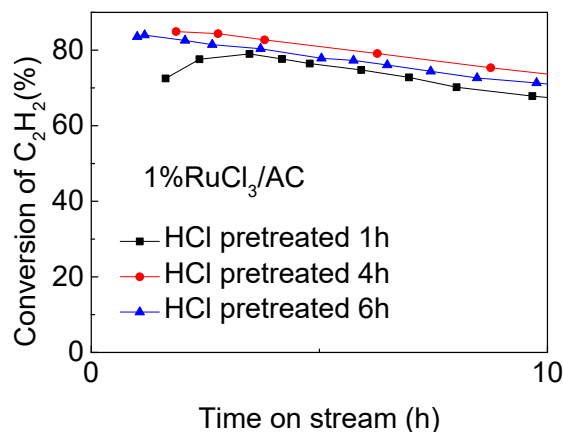
Figure S9 (A) The conversion of acetylene in acetylene hydrochlorination over RuCl$_3$/AC catalysts for different HCl activation time; Reaction conditions: T = 180 ^{o}C, GHSV(C$_2$H$_2$) = 180 h^{-1} and V$_{HCl}$/V$_{C2H2}$ = 1.10.
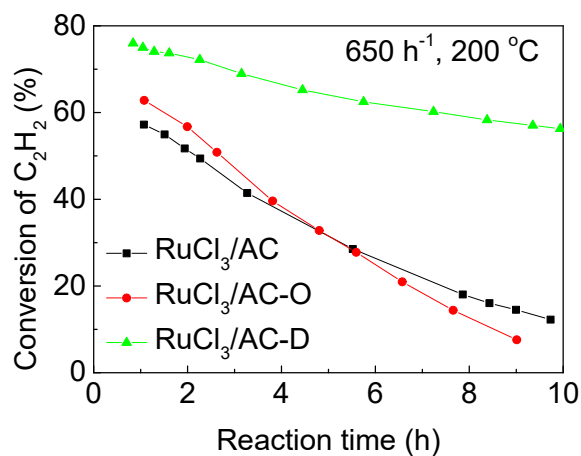
Figure S10. The conversion of acetylene in acetylene hydrochlorination over RuCl$_3$/AC, RuCl$_3$/AC-O and RuCl$_3$/AC-D. Reaction conditions: Pressure: 0.1 MPa, T= 200 ^{o}C, GHSV(C$_2$H$_2$) = 650 h^{-1} and V$_{HCl}$/V$_{C2H2}$= 1.10.
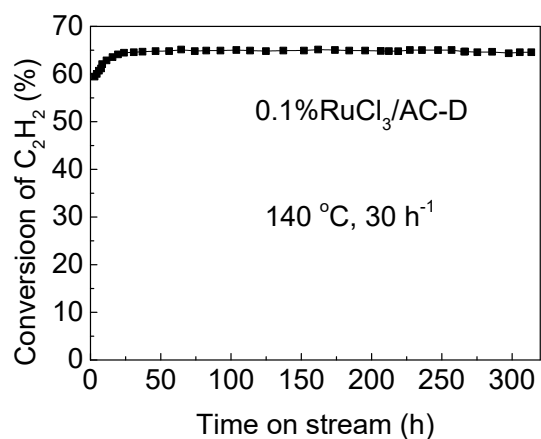
Figure S11. The life time of 0.1% RuCl$_3$/AC-D in acetylene hydrochlorination. Reaction conditions: Pressure: 0.1 MPa, T= 140 °C, GHSV(C$_2$H$_2$) = 30 h^{-1} and V$_{HCl}$/V$_{C2H2}$= 1.10.
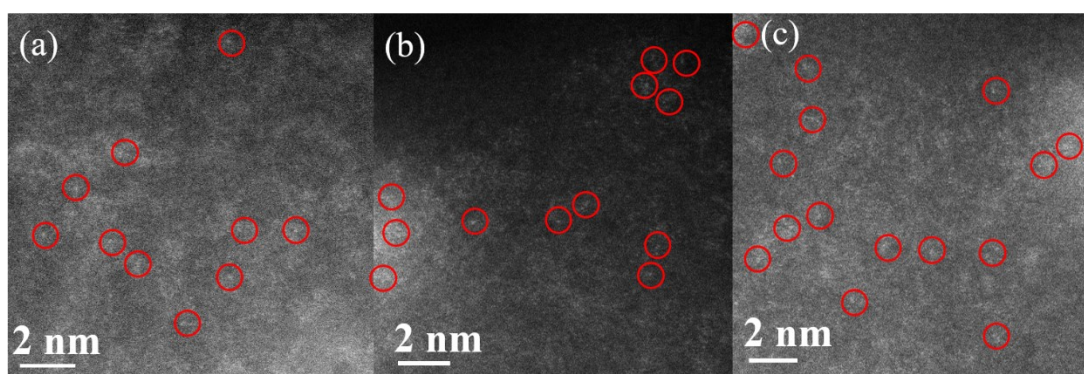
Figure S12. HAADF-STEM images of (a) RuCl$_3$/AC-used, (b) RuCl$_3$/AC-O-used and (c) RuCl$_3$/AC-D-used.
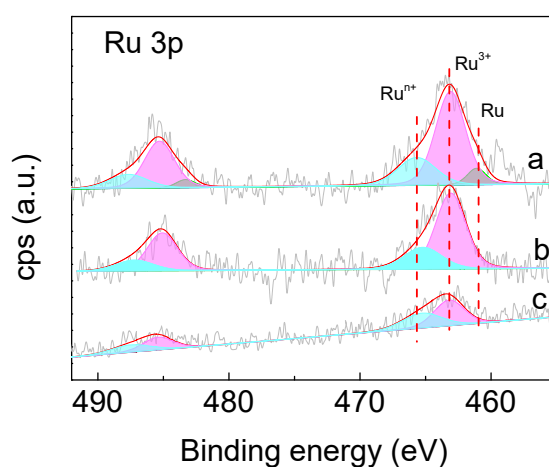
Figure S13. XPS of Ru 3p for (a) RuCl$_3$/AC-used, (b) RuCl$_3$/AC-D-used and (c) RuCl$_3$/AC-O-used.
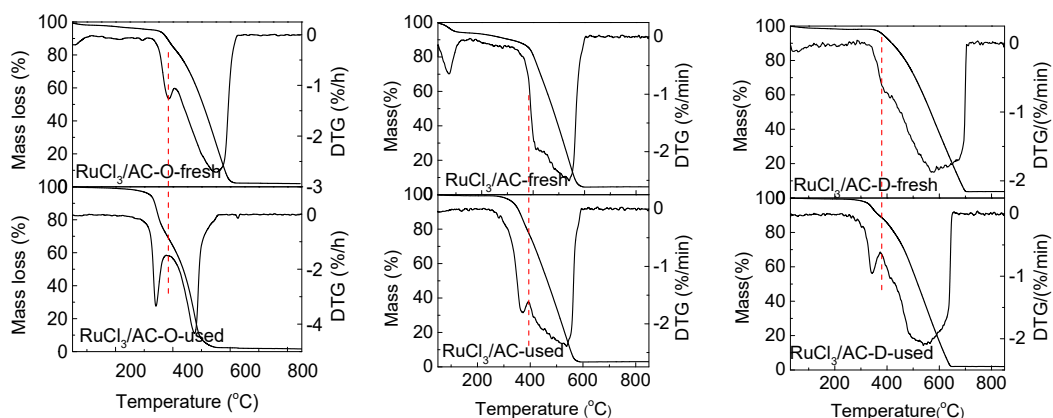
Figure S14. TG and DTG profiles for fresh and used RuCl$_3$/AC, RuCl$_3$/AC-O and RuCl$_3$/AC-D catalysts under air flow.
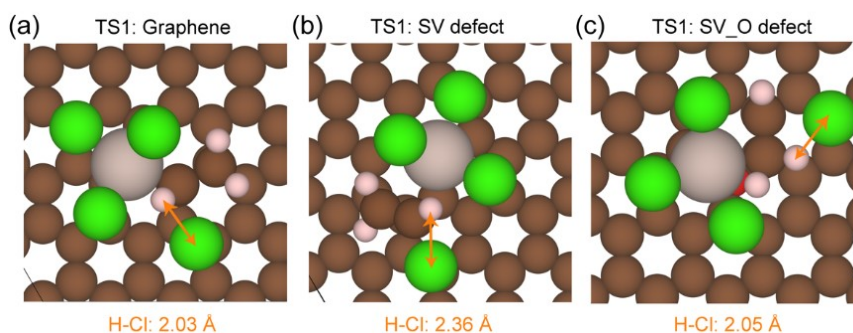
Figure S15. The optimized transition-state (TS1) intermediate structures for C$_2$H$_2$ hydrochlorination at RuCl$_3$ with different carbon structures.
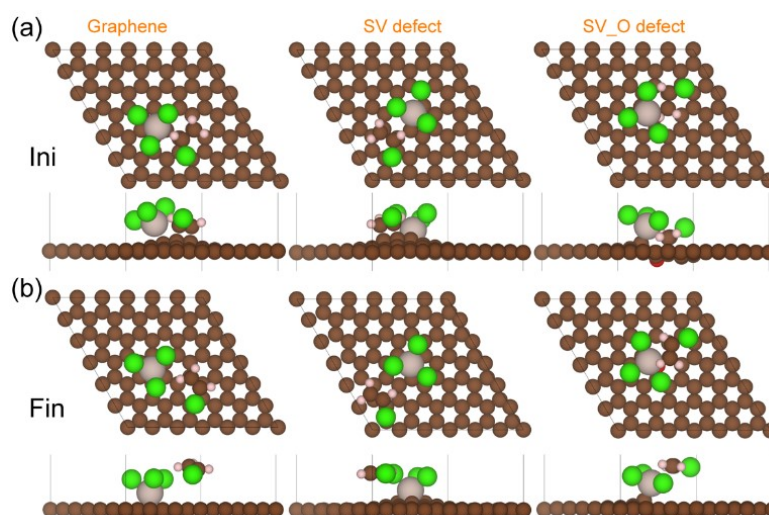
Figure S16. The optimized (a) initial and (b) final structures for desorption process (TS2) at RuCl$_3$ with different carbon structures.
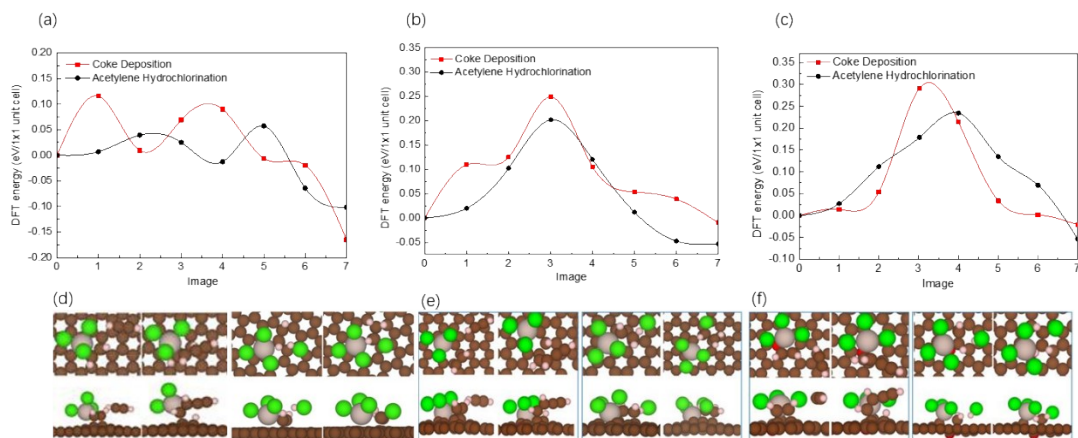
Fig S17. Minimum energy paths of acetylene polymerization ($C_2H_2+C_2H_2 = C_4H_4$) and acetylene hydrochlorination reactions on (a) RuCl$_3$@graphene, (b) RuCl$_3$@SV-O and (c) RuCl$_3$@SV and the optimized initial and final structures of acetylene polymerization and acetylene hydrochlorination reactions on (d) RuCl$_3$@graphene, (e) RuCl$_3$@SV-O and (f) RuCl$_3$@SV.

Table S1. Texture properties of active carbon and ruthenium catalysts

Catalysts	ACs		Catalysts		O^a/ at. %
	S.A. ($m^2·g^{-1}$)	P.V. ($cm^3·g^{-1}$)	S.A. ($m^2·g^{-1}$)	P.V. ($cm^3·g^{-1}$)	
RuCl₃/AC	1235	0.53	1109	0.47	5.8
RuCl₃/AC-O	1106	0.50	1104	0.51	13.7
RuCl₃/AC-D	1234	0.56	1190	0.57	1.4

O^a: surface atomic concentrations of Ru catalysts determined by XPS.

Table S2. Adsorption Energy and Charge of RuCl₃ at Different Adsorption sites

Configuration	Adsorption energy of RuCl₃(eV) on carbon	Border Charge
graphene	-0.65	0.91
graphene-OH	-0.64	0.94
graphene-O	-1.00	1.12
graphene -COOH	-0.68	0.96
DV	-0.42	0.92
SW	-0.67	0.93
SV	-1.53	0.76
SV-OH	-1.32	0.94
SV-O	-0.41	0.94
SV-COOH	-0.15	1.05

Table S3. X-ray photoelectron measurements (XPS) spectra fitting results of Ru 3p for the used ruthenium catalysts

Samples	Ru^0 461.3 eV	Ru^{3+} 463.3 eV	Ru^{n+} 465.0 eV
RuCl₃/AC-used	7.4	67.2	25.4
RuCl₃/AC-O-used	-	57.1	42.9
RuCl₃/AC-D-used	-	73.5	26.5

Table S4. Calculated binding energies of HCl and C₂H₂ on RuCl₃ with different carbon structures. Energies are in eV/1 × 1 unit cell.

Carbon structures	E_{b-HCl}	E_{b-C2H2}
RuCl₃@SV	-0.75	-2.42
RuCl₃@SV-O	-0.82	-3.18
RuCl₃@graphene	-0.96	-2.67

Table S5. Comparison of Ru-based catalyst in acetylene hydrochlorination

Catalyst	Ru (wt.%)	V_{cat} (mL)	W_{cat} (g)	T_{bed} (°C)	GHSV(C_2H_2) (h^{-1})	V_{HCl}/V_{C2H2}	Conversion (%)	Reference
$RuCl_3$/AC-D	1	2	0.93	180	180	1.10	100	This work
$RuCl_3$/AC-D	1	0.6	0.28	200	650	1.10	76	This work
AC-D	n.a.[a]	0.6	0.28	200	650	1.10	10	This work
Ru/NC-g	1	0.5	0.25	200	650	1.10	95	[1]
NC-g	n.a.[a]	0.5	0.25	200	650	1.10	34	[1]
Ru@TPPB/AC	1	5	n.a.[a]	180	360	1.15	100	[2]
Ru–O/AC–O	1	2	n.a.[a]	180	180	1.15	100	[3]
TPAP/AC-HCl	1	2	n.a.[a]	180	180	1.15	97	[4]
Ru/AC-NHN	1	2	n.a.[a]	180	360	1.15	94	[5]
Ru/SAC-C300	1	n.a.[a]	n.a.[a]	170	180	1.10	96	[6]

[a] n.a.: not available.

References:

1   S. Kaiser, R. Lin, F. Krumeich, O. Safonova, J. Pérez-Ramírez, Preserved in a Shell: High-Performance Graphene-Confined Ruthenium Nanoparticles in Acetylene Hydrochlorination, *Angew. Chem. Int. Ed.* 2019, **58**, 2-10.

2   S. Shang, W. Zhao, Y. Wang, X. Li, J. Zhang, Y. Han, W. Li, Highly Efficient Ru@IL/AC To Substitute Mercuric Catalyst for Acetylene Hydrochlorination, *ACS Catal.* 2017, **7**, 3510-3520.

3   B. Man, H. Zhang, J. Zhang, X. Li, N. Xu, H. Dai, M. Zhu, B. Dai, Oxidation Modification of Ru-Based Catalyst for Acetylene Hydrochlorination, *RSC Adv.* 2017, **7**, 23742-23750.

4   X. Li, H. Zhang, B. Man, L. Hou, C. Zhang, H. Dai, M. Zhu, B. Dai, Y. Dong, J. Zhang, Activated Carbon-Supported Tetrapropylammonium Perruthenate Catalysts for Acetylene Hydrochlorination, *Catalysts*. 2017, **7**, 311.

5   N, Xu, M, Zhu, J, Zhang, H, Zhang, B, Dai, Nitrogen Functional Groups on an Activated

Carbon Surface to Effect The Ruthenium Catalysts in Acetylene Hydrochlorination, *RSC Adv.* 2015, **5**, 86172-86178.

6   Y, Pu, J, Zhang, L, Yu, Y, Jin, W, Li, Active Ruthenium Species in Acetylene Hydrochlorination, *Appl. Catal., A.* 2014, **488**, 28-36.